

# Predicting and Designing for the Impact of Process Variations and Mismatch on the Trim Range and Yield of Bandgap References

Vishal Gupta, *Student Member, IEEE* and Gabriel A. Rincón-Mora, *Senior Member, IEEE*  
GT Analog and Power IC Design Lab, Georgia Institute of Technology, Atlanta, GA

## Abstract

*Process tolerance and device mismatch produce significant random variations in bandgap voltage reference circuits. These variations lead to errors in the reference voltage and significantly impact manufacturing cost by increasing trimming requirements and decreasing yield. Current-mirror mismatch, followed by  $V_{BE}$  spread, package shift, and resistor mismatch are the dominant sources of random error in bandgap reference circuits. A folded-cascode topology, often used in low voltage applications, can be optimized to effectively alleviate the effects of a mismatch in the mirroring devices. By decreasing the ratio of the current in the cascode to that of the bandgap core circuit and ascertaining the best-matched devices for implementing current-mirrors and current sources, these mismatches can be significantly reduced.*

## 1. Introduction

Bandgap references are high-performance analog circuits that find applications in a host of analog [1], digital [2], and mixed-signal [3] integrated systems. For all these applications, the accuracy of the bandgap reference voltage is crucial as it can severely limit system functionality. This is especially so in the case of sensitive blocks like sensors and A/D converters [3]. Considerable work has been done to protect the reference voltage from variations in supply [2], [4], [5] and temperature [1], [3], [4], [6], [7]. However, process variations, which arise from tolerance and mismatch, can degrade the accuracy of the most well-designed bandgap reference and hence need careful attention [1], [4], [8] which is why trim circuits are used. These process-induced errors in the reference voltage raise the required trim-range (number of trim bits) for a specified accuracy performance, thereby directly affecting cost by lowering yield and increasing test time. Hence, quantifying and designing for the effect of the various sources of error that degrade the accuracy of bandgap references is crucial to predict trim range and yield.

This work presents the bandgap reference designer with analytical expressions for the impact of process variations on the bandgap voltage, and their implications on bandgap reference design and trim range. The analysis

presented is applicable to most bandgap-based circuits. For clarity and convenience, the analysis is performed within the context of the bandgap's basic building block (described in Section II). Given the conclusions drawn in Section II, a practical bandgap reference topology (described in Section III) is designed and optimized to minimize the critical error sources. The final conclusions are presented in Section IV.

## 2. Analysis of Process-Induced Errors

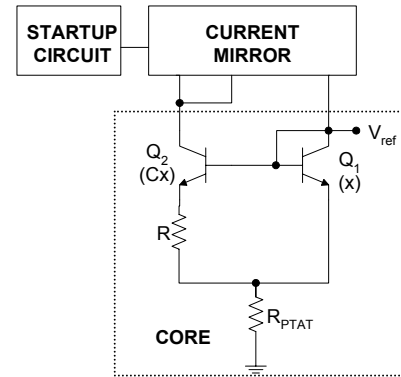


Fig. 1. Basic bandgap reference cell.

The basic topology of the circuit used for the analysis of error sources in bandgap references is shown in Fig. 1. This is the building block for most bandgap reference circuits [3], [4], [7], [8] and the expressions for the error in the reference voltage of this circuit can easily be applied to most practical bandgap implementations. Referring to Fig. 1, the reference voltage generated by the first-order bandgap reference is generally given by

$$\begin{aligned} V_{\text{ref}} &= V_{\text{BE1}} + V_{\text{PTAT}} = V_{\text{BE1}} + 2I_{\text{PTAT}} R_{\text{PTAT}} \\ &= V_{\text{BE1}} + 2 \frac{V_t \ln C}{R} R_{\text{PTAT}}, \end{aligned} \quad (1)$$

and, consequently,

$$\Delta V_{\text{ref}} = \Delta V_{\text{BE1}} + 2\Delta I_{\text{PTAT}} R_{\text{PTAT}}, \quad (2)$$

where  $V_{\text{PTAT}}$  is the Proportional to Absolute Temperature (PTAT) component of the reference voltage,  $I_{\text{PTAT}}$  is the PTAT current, and  $C$  is the ratio of the current densities of  $Q_1$  and  $Q_2$ . A  $\Delta$  symbol indicates a change in the variable that follows it. The factor of '2' arises since the current through  $R_{\text{PTAT}}$  is the sum of the PTAT currents flowing through  $Q_1$  and  $Q_2$  and this value will change from circuit to circuit. The magnitude of the error in the reference voltage ( $\Delta V_{\text{ref}}$ ) is obtained by comparing the

reference voltage of an “ideal” bandgap circuit to that in which the particular error source being studied is artificially introduced. The mathematical analysis of the error sources is presented in [8]. The analysis of current-mirror mismatch, a critical source of error, has been presented in the Appendix as an example of the analysis.

## 2.1 Sources of Errors

*Current Mirror Mismatch:* This error arises from the deviation in the required ratio of the mirror currents. This deviation may arise from various factors, like W/L mismatch, threshold voltage ( $V_T$ ) mismatch, lambda effects of MOS devices, resistor mismatch, and area mismatch of bipolar devices. Using (A1)-(A8), for a mismatch of  $\delta_M$  between the mirror currents,

$$\Delta V_{\text{ref}} = V_t \delta_M \left( 1 + \frac{1}{\ln C} \right) + \frac{V_t}{R} \left[ 2\delta_M + \ln C \left( 1 + \frac{\delta_M}{\ln C} \right) \delta_M \right] R_{\text{PTAT}}. \quad (3)$$

*Resistor Mismatch:* Though resistors can be matched to a high degree of accuracy (typically 1%), resistor mismatch influences the PTAT voltage, which is a strong function of the ratio of the resistors  $R_{\text{PTAT}}$  and  $R$ . From [8], a  $\delta_{\text{RR}}$  mismatch in these resistors leads to

$$\Delta V_{\text{ref}} = 2 \frac{V_t \ln C}{R} R_{\text{PTAT}} \delta_{\text{RR}} = V_{\text{PTAT}} \delta_{\text{RR}}. \quad (4)$$

*Resistor Tolerance:* Process variations can lead to a large deviation of resistor values (often as large as 20%). This variation changes the  $V_{\text{BE}}$  component by altering the PTAT current flowing in the circuit. If  $\delta_{\text{RA}}$  is the fractional deviation of the resistors from their nominal value, from [8], we can see that the expression for the error in  $V_{\text{ref}}$  is given by

$$\Delta V_{\text{ref}} = -V_t \delta_{\text{RA}}. \quad (5)$$

*Transistor Mismatch:* These errors result from a deviation in the desired ratio of the areas of transistors  $Q_1$  and  $Q_2$ . From [8], if  $\delta_{\text{NPN}}$  is the fractional error in the ratio, the error in the reference voltage is given by

$$\begin{aligned} \Delta V_{\text{ref}} &= \frac{V_t \delta_{\text{NPN}}}{\ln C} + 2 \frac{V_t}{R} R_{\text{PTAT}} \delta_{\text{NPN}} \\ &= \frac{1}{\ln C} (V_t + V_{\text{PTAT}}) \delta_{\text{NPN}}. \end{aligned} \quad (6)$$

*Other Error Sources:* Other large sources of error are  $V_{\text{BE}}$  spread and package shift. The spread in the base-emitter voltage of the bipolar transistors is a considerable source of error and is critical because it directly translates to an error in the bandgap reference voltage. Package shift (a deviation in the reference voltage caused by the local and die-wide mechanical stresses of a package on its IC) is a

post-package error that can only be effectively eliminated by post-package trimming techniques [1], [11]. Errors due to Early voltage effects between the two bipolar devices have non-linear temperature dependence and, consequently, cannot be trimmed. However, they can be significantly mitigated through circuit design techniques whereby the collector voltages of the bipolar devices,  $Q_1$  and  $Q_2$ , are forced to be equal [1]-[8].

## 2.2 Relative Magnitude

Table 1 presents a summary of the various sources of error in a bandgap reference circuit and their typical 3- $\sigma$  magnitudes along with qualitative comparison. The application of the results of the error source analysis to a practical bandgap reference topology and its close agreement with simulated data over a wide temperature range can be obtained in [8]. In [8], the 3- $\sigma$  offset in the reference voltage caused by current-mirror mismatch proved to be the dominant error in a bandgap reference. This is primarily due to the high mismatch characteristic of MOS transistors, which are often used to implement current-mirrors. In MOS devices, drain-current mismatch can be as high as 10% [9]. In general, MOS devices do not match as well as bipolars (~2%), which in turn exhibit a higher mismatch than resistors (~1%) [10]. Hence, current-mirror mismatch,  $V_{\text{BE}}$  spread, package shift, and resistor mismatch have the largest impact on trim range.

**Table 1. Principle features of the various error sources in bandgap references.**

Error	Typical Value (3- $\sigma$ )	Relative Magnitude of Effect	Trimnable	Temp. Dependence
Current-Mirror Mismatch	$\pm 1\%$ - 10%	Very Large	Yes	Linear
Resistor Mismatch	$\pm 1\%$	Large	Yes	Linear
Resistor Tolerance	$\pm 20\%$	Small	Yes	Linear
Transistor Mismatch	$\pm 1\%$	Small	Yes	Linear
$V_{\text{BE}}$ spread	$\pm 24$ mV	Very Large	Yes	Linear
Package Shift	$\pm 5 - 7$ mV	Large	No	Non-linear
Early voltage, lambda	50V, 0.1	Small	No	Non-linear

## 2.3 Discussion – Trimmability and Layout Implications of Errors

As (3)-(6) reveal, the errors due to resistor mismatch, resistor tolerance, and transistor mismatch, exhibit linear

temperature dependence. Hence, they can be eliminated by trimming, which inherently cancels first order errors because it alters the PTAT voltage to account for their effects. The error due to current-mirror mismatch is also trimmable if the current mismatch ( $\delta_M$ ) is not temperature dependent. However, trimming is an expensive and time-consuming process, and a reduction in the trim range required for a bandgap reference is desired for lower test times and higher yield.

Errors due to resistor mismatch and transistor mismatch can only be reduced through layout techniques (such as common centroid layout and dummy devices). Errors due to resistor tolerance can be reduced by choosing a material for the resistor that does not exhibit significant spread in resistivity over process, voltage, and temperature. Polysilicon resistors, for example, typically exhibit a smaller variation of resistance with voltage and temperature, than n-well resistors. Further, though current-mirror mismatch errors can be significantly mitigated through careful layout, they can also be attenuated through judicious circuit design practices. Section 3 describes one such design methodology.

### 3. Reducing the Effects of Current-Mirror Mismatch in a Practical Design

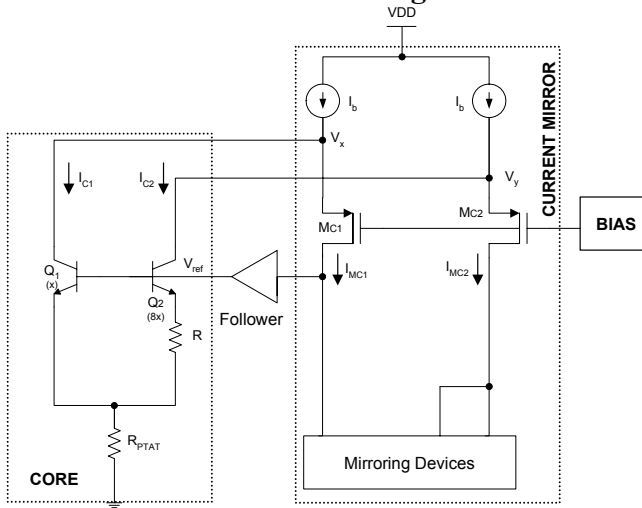


Fig. 2. Block diagram of bandgap reference.

The folded topology is a well-known structure that is often used in low-voltage circuits. Fig. 2 presents the basic architecture of the bandgap reference under discussion, where a folded-cascode is used as a feedback error amplifier. Here, the shunt feedback from the folded-cascode amplifier decreases the output impedance of the bandgap, a critical specification for load regulation and shunting noise. However, within the context of a

bandgap circuit, the entire folded-cascode structure functions as the effective current-mirror of the bandgap core.

Due to emitter degeneration, the transconductance of the bandgap cell ( $Q_1$  and  $Q_2$ ) is much lower than the transconductance of a conventional input differential pair. This makes the bandgap reference extremely vulnerable to current-mirror mismatch, which produces large voltage offsets in the core. Hence, although a folded-cascode or Norton amplifier topology is well known, its design constrictions and tradeoffs differ in bandgap circuits, which are extremely sensitive to mismatch of the collector currents of the bipolar transistors ( $Q_1$  and  $Q_2$ ). In other words, the folded-cascode amplifier has to be optimized for low offsets.

#### 3.1 Designing for Current-Mirror Mismatch

*Proportioning the Currents:* In the circuit of Fig. 1, if the current mirror is simply implemented using PMOS devices connected to the supply, a mismatch in the mirror currents directly causes a mismatch in the core collector currents. Thus, to reduce current-mirror mismatch errors, a technique is needed to desensitize the mismatch in the core currents to those of the mirroring devices. In Fig. 2, consider a mismatch in the currents through cascodes,  $M_{C1}$  and  $M_{C2}$ , which will lead to a difference in their absolute values. This difference, or surplus current, will be reflected as the difference between the currents in the core, i.e., the collector currents of  $Q_1$  and  $Q_2$ . Now, if these core currents are higher than the currents in the cascodes, the percentage mismatch of the core currents will be lower than the percentage mismatch in the cascode currents. Further, if the core currents are raised while keeping the cascode currents constant, the same absolute (and fractional) mismatch in the cascodes will now produce an even smaller fractional mismatch in the core. Mathematically,

$$\begin{aligned} I_b &= I_{MC2} + I_{C2} = I_{MC1} + I_{C1} \\ \Rightarrow I_{MC2} + I_{C2} &= I_{MC2}(1 + \delta_{\text{mirr}}) + I_{C2}(1 - \delta_M), \\ \Rightarrow \delta_M &= \delta_{\text{mirr}} \frac{I_{MC2}}{I_{C2}} = \delta_{\text{mirr}} K_1, \end{aligned} \quad (7)$$

where  $\delta_M$  and  $\delta_{\text{mirr}}$  are the fractional mismatches in the currents in the core bipolar devices and the mirror cascodes, respectively, and  $K_1$  is the ratio of the current in the cascode to that in the core. Thus, by lowering the ratio  $K_1$ , the same fractional mismatch between the currents in the cascodes (and hence the mirroring devices),  $\delta_{\text{mirr}}$ , produces a smaller mismatch in the core,  $\delta_M$ . Hence, through a folded topology, the mismatch between the current-mirror devices is effectively *attenuated*.

The benefits of the folded topology, and hence of (7), have costs and limits. Note that current-mirror mismatch in the circuit of Fig. 2 stems from a mismatch in three pairs of devices, namely, mismatch in the  $I_b$ -current sources ( $\Delta V_{\text{ref-}I_b}$ ),  $V_T$  mismatch between the cascoding devices  $M_{C1}$  and  $M_{C2}$  ( $\Delta V_{\text{ref-}V_T}$ ), and mismatch in defining mirroring devices themselves ( $\Delta V_{\text{ref-mir}}$ ). It is reasonable to expect the total current-mirror mismatch error to approximately equal the root sum squared (RSS) of these individual random errors, i.e.,

$$\Delta V_{\text{ref}} \approx \sqrt{(\Delta V_{\text{ref-}I_b})^2 + (\Delta V_{\text{ref-}V_T})^2 + (\Delta V_{\text{ref-mir}})^2}. \quad (8)$$

Thus, a reduction in the error predicted by (7) would only prove effective if mismatch error of the mirroring devices is dominant. Fig. 3 shows how the total induced error decreases with the ratio  $K_I$ . The error reduces proportionally till it reaches the “floor” set by  $V_T$  mismatch errors.

Further, the cascodes and mirroring devices form a high-gain amplifier that equalizes the collector voltages of the bipolars through feedback. Hence, decreasing the cascode current to very low levels would decrease finite gain errors caused by this amplifier by increasing the loop gain, but would also increase  $\delta_{\text{mirr}}$  and the  $V_T$  mismatch [9]. Thus, in order to obtain the attenuation predicted by (7), a sufficiently high current in the cascode would be required, with a correspondingly larger current in the core, leading to the tradeoff of larger power dissipation for improved accuracy.

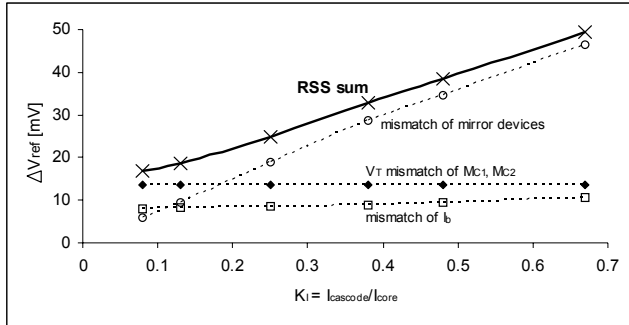


**Fig. 3. Current-mirror mismatch error and its relation to the ratio of the current in the cascode to the core ( $K_I$ ).**

*Implementing the  $I_b$ -current Sources:* The  $I_b$ -current sources in Fig. 2 play a crucial role in the bandgap reference. The devices used to implement these sources should be extremely well matched to reduce current-mirror mismatch errors. A mismatch in these devices can decrease the effectiveness of folding the currents (shown in (7)) and can also cause its own current-mirror mismatch, even if the cascodes and mirroring devices are well-matched. On the other hand, increasing the output

resistance of these current sources reduces the sensitivity of the bandgap core to  $V_T$  and  $K'$  mismatches of cascoding devices  $M_{C1}$  and  $M_{C2}$  (a higher output resistance increases the source-degenerating effects on  $M_{C1}$  and  $M_{C2}$ ).

Resistors often exhibit superior matching properties to MOS devices. The latter, however, have higher output resistance. Thus, a delicate tradeoff exists in the design of the  $I_b$ -current sources, and the designer must therefore ascertain how these devices will match before making a design decision. For example, consider a 300 mV voltage drop across the  $I_b$ -current sources, a 1% resistor mismatch ( $R_{\text{mis}}$ ), 2% transconductance parameter mismatch ( $K'_{\text{mis}}$ ), 2% W/L mismatch ( $W/L_{\text{mis}}$ ), and a 10 mV threshold voltage mismatch ( $V_{T\text{-mis}}$ ). The current through the  $I_b$ -current sources implemented as resistors would depend on the magnitude of their resistance and the voltage across them. Hence, the mismatch between the  $I_b$ -current sources if they are implemented as resistors, ( $I_{b\text{-mis-R}}$ ), would be a root sum squared (RSS) of the random mismatch in the resistor values and of the voltage across them. Thus,

$$\begin{aligned} I_{b\text{-mis-R}} &\approx \sqrt{(R_{\text{mis}})^2 + (V_{T\text{-mis}})^2} \\ &= \sqrt{(1\%)^2 + \left(\frac{10}{300} \times 100\right)^2} \approx 3\%. \quad (9) \end{aligned}$$

Assuming MOS devices, the mismatch ( $I_{b\text{-mis-MOS}}$ ) is given by the RSS of the mismatch between transconductance parameter,  $K'$ , W/L ratio, and threshold voltage,  $V_T$ . Hence,

$$\begin{aligned} I_{b\text{-mis-MOS}} &\approx \sqrt{(K'_{\text{mis}})^2 + (W/L_{\text{mis}})^2 + (2V_{T\text{-mis}})^2} \\ &\approx \sqrt{(2\%)^2 + (2\%)^2 + \left(2 \times \frac{10}{300} \times 100\right)^2} \approx 6\%. \quad (10) \end{aligned}$$

The overdrive voltage can be increased to attenuate the effect of  $V_T$  mismatch [10], at the cost of voltage headroom and current consumption. The factor of “2” arises for the  $V_T$  mismatch term because it is assumed that the MOS devices used to implement the current sources are operating in the saturation regime, where the drain current is proportional to the square of the overdrive voltage, or difference between the gate-source and threshold voltage. Intuitively, this can be seen by viewing the square overdrive term as two terms, each depending on  $V_T$ , and thereby doubling its mismatch effect.

Mismatches due to lambda effects and other MOS parameters (that have been ignored in (10)) further degrade the matching performance of these devices. Consequently, resistors would be a better design choice in implementing the  $I_b$ -current sources (balancing matching versus source-degenerating performance). Ultimately,

mismatches between the  $I_b$ -current sources can be notably reduced through the use of dynamic element matching (DEM) techniques [12], [13], which have an implied cost of complexity, die size, and noise. This would significantly reduce the  $\Delta V_{ref-Ib}$  and  $\Delta V_{ref-VT}$  terms in (8).

*Implementing the Current-Mirror:* The implementation of the current-mirror itself is critical and careful attention must be paid to its accurate and robust implementation. The designer must ascertain the best-matched devices available, in a manner similar to the procedure for choosing the  $I_b$ -current sources.

### 3.2 Complete Circuit Description and Simulation Results

Fig. 4 presents the complete schematic of the proposed bandgap reference. High- $\beta$  NPN devices,  $Q_3$  and  $Q_4$ , along with their degenerating resistors,  $R_3$  and  $R_4$ , form a well-matched, high output impedance current-mirror. Transistors  $Q_{FN}$  and  $Q_{FP}$  create a super-beta voltage follower, i.e., unity-gain buffer which is used to close the feedback loop and prevent the bandgap core from loading the current-mirror. Transistor  $M_{FOLL}$  provides the bias current for the super- $\beta$  buffer. Finally, capacitor  $C$  establishes the dominant pole and hence the loop bandwidth of the circuit. Table 2 presents the simulated functional specifications of the circuit. Standard models compatible with 1.5 $\mu$ m process obtained from MOSIS were used for the simulations.

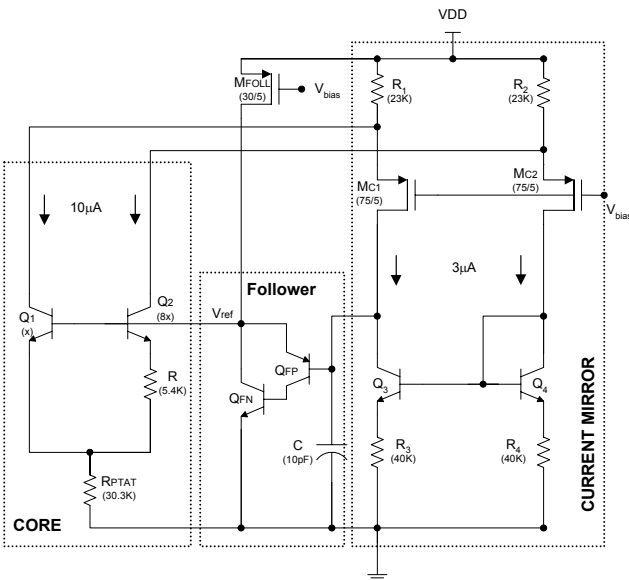


**Fig. 4. Circuit embodiment of a high-accuracy bandgap reference.**

Table 3 presents a quantitative summary of the offsets induced by various random sources of error on the

bandgap voltage and their comparison with their analytical counterparts. As can be seen, the two are in excellent agreement. The temperature drift of the current-mirror mismatch, now primarily caused by the  $V_T$  mismatch between the cascoding devices (since NPN devices and resistors can be matched to within 2%), depends on the temperature coefficient of the  $V_T$  mismatch, and hence this error is typically not trimmable. It can be minimized by increasing the flow of current through the cascoding devices to minimize their mismatch, but that implies an increased current in the core to reduce mirror-imposed offsets. Further, 24 mV spread in the base-emitter voltage of the NPN devices is based on experience and takes into account worst-case process variations – it is now the primary factor that determines the trim range of the bandgap reference. The calculated trim-range is approximately  $\pm 35$  mV (70 mV full-scale).

**Table 2. Simulated circuit characteristics.**

Circuit Parameter	Simulated Value
$V_{ref} (@ T=27^\circ C)$	1.23 V
Minimum supply voltage	1.41 V
T.C. performance (after trim)	0.34 %
Quiescent Current	60 $\mu A$
Line regulation	1.27 mV/V
Power Supply Rejection (@100 Hz)	-55 dB

**Table 3. Comparison of Simulated and Analytical Results for Error Sources (at 25  $^\circ C$ ).**

Type of Error	3- $\sigma$ -Error in Devices	Simulated $\Delta V_{ref}$ [mV]	Analytical $\Delta V_{ref}$ [mV]
Current Mirror Mismatch	$\pm 2\%$ NPN mismatch, $\pm 1\%$ Resistor mismatch, $\pm 5$ mV $V_T$ mismatch	$\pm 18.5$	$\pm 16.9$
Resistor Mismatch	$\pm 1\%$	$\pm 6.3$	$\pm 6.4$
Transistor Mismatch	$\pm 2\%$	$\pm 6.0$	$\pm 6.0$
Resistor Tolerance	$\pm 20\%$	$\pm 5.2$	$\pm 5.1$
$\Delta V_{be}$		$\pm 24.0$ mV	
Package Shift		$\pm 7$ mV	
<b>RMS Error</b>	$\sqrt{\Delta V_{ref_i}^2}$ [mV]	<b><math>\pm 32.7</math></b>	<b><math>\pm 31.8</math></b>
<b>Trim-range</b>	<b>Full-scale <math>\approx 2x</math> RMS [mV]</b>	<b>65.4</b>	<b>63.6</b>

## 4. Conclusions

The analytical expressions obtained for various sources

of error allow a designer to quantitatively ascertain the impact of process variations on the trim range of a bandgap reference. Current-mirror mismatch, which causes a mismatch in the collector currents of the bipolar transistors in the core of the bandgap reference, is the dominant source of error. This mismatch is a combination of various errors, namely, Early voltage, lambda effects, W/L mismatch, resistor mismatch, and  $V_T$  mismatch. A folded topology is therefore used to decouple the biasing currents, and therefore the effects of the mirror devices, from the bandgap core. Once decoupled, the design is optimized by reducing the ratio of the current in the cascode to that in the core. In general, current sources and mirrors must be implemented using best-matched devices available, after ascertaining the trade-offs between matching, output resistance, current consumption, and required voltage headroom. Hence, though process variations can significantly influence the trim range and yield of bandgap references, the analysis and circuit design principles presented allow the designer to predict and considerably attenuate their deleterious effects.

## Appendix

In the analyses presented, the variable subscripted by ‘x’ represents the erroneous quantity. For example,  $I_{PTAT-x}$  represents the erroneous PTAT current. Further, the symbol  $\Delta$  followed by a quantity represents the variation error in that quantity. For example,  $\Delta V_{ref}$  represents the variation of  $V_{ref}$  from ideality.

The base-emitter voltage of a transistor is given by

$$V_{BE} = V_t \ln \left( \frac{I_C}{J_S \cdot \text{Area}} \right), \quad (\text{A1})$$

where  $I_C$  and  $J_S$  is the collector current and reverse saturation current per unit area of the transistor. The PTAT current is

$$I_{PTAT} \equiv I_{C2} = \frac{V_t}{R} \ln \left( C \cdot \frac{I_{C1}}{I_{C2}} \right), \quad (\text{A2})$$

where  $C$  is the ratio of the areas of transistors  $Q_1$  to  $Q_2$ , and  $I_{C1}$  and  $I_{C2}$  are their collector currents, respectively.

**Current Mirror Mismatch:** A mismatch in any one of the transistors of the current mirror changes the current in all the branches of the circuit. Assuming a mismatch of  $\delta_M$  in the mirror currents ( $I_{C1} = (1+\delta_M)I_{C2}$ , where  $I_{C1}$  and  $I_{C2}$  are the mirror currents flowing in  $Q_1$  and  $Q_2$ , respectively) and using (A2), the erroneous PTAT current is

$$I_{PTAT-x} = \frac{V_t}{R} \ln \left[ \frac{I_{C2}(1+\delta_M)C}{I_{C2}} \right] = \frac{V_t}{R} \ln C + \frac{V_t}{R} \ln(1+\delta_M)$$

$$\approx I_{PTAT} + \frac{V_t}{R} \delta_M. \quad (\text{A3})$$

$$\Rightarrow \Delta I_1 = \frac{V_t}{R} \delta_M, \quad (\text{A4})$$

where  $\Delta I_1$  is the error in the current flowing through both branches. The current through  $Q_1$  has a further error due to the actual mismatch of the current mirror,

$$\begin{aligned} \Delta I_1 &= I_{PTAT-x} \delta_M = \frac{V_t}{R} \ln[(1+\delta_M)C] \delta_M \\ &\approx \frac{V_t}{R} \ln C \left( 1 + \frac{\delta_M}{\ln C} \right) \delta_M, \end{aligned} \quad (\text{A5})$$

From (A1),

$$\begin{aligned} \Delta V_{BE1} &= V_t \ln \left[ \frac{I_{PTAT-x}(1+\delta_M)}{I_{PTAT}} \right] \\ &= V_t \ln \left[ (1+\delta_M) \frac{\ln(1+\delta_M)C}{\ln C} \right], \end{aligned} \quad (\text{A6})$$

$$\Rightarrow \Delta V_{BE1} \approx V_T \delta_M \left( 1 + \frac{1}{\ln C} \right). \quad (\text{A7})$$

Consequently,

$$\Delta V_{ref} = \Delta V_{BE1} + (2\Delta I_1 + \Delta I_2) R_{PTAT}. \quad (\text{A8})$$

## References

- [1] G. Meijer, G. Wang, and F. Fruett, “Temperature sensors and voltage references implemented in CMOS technology,” *IEEE Sensors*, vol. 1, pp. 225-234, Oct. 2001.
- [2] K. Tham, K. Nagaraj, “A low-voltage high PSRR voltage reference in CMOS process,” *IEEE J. Solid-State Circuits*, vol. 5, pp. 586-590, May 1995.
- [3] P.E. Allen and D. R. Holberg, *CMOS Analog Circuit Design*, Oxford Univ. Press, 2002, pp. 612-698.
- [4] G.A. Rincón-Mora, *Voltage References*, IEEE Press, John Wiley & Sons, Inc., 2002.
- [5] G. Giustolisi and G. Palumbo, “A detailed analysis of power-supply noise attenuation in bandgap voltage references,” *IEEE Trans. Circuits Sys. - I*, vol. 50, pp. 185-197, Feb. 2003.
- [6] K.E. Kujik, “A precision reference voltage source,” *IEEE J. Solid-State Circuits*, Vol. SC-6, pp. 2-7, June 1973.
- [7] A.P. Brokaw, “A simple three-terminal IC bandgap reference,” *IEEE J. Solid-State Circuits*, vol. SC-9, pp. 388-393, Dec. 1974.
- [8] V. Gupta and G.A. Rincón-Mora, “Predicting the effects of error sources in bandgap reference circuits and evaluating their design implications,” in *Proc. 45<sup>th</sup> MWSCAS*, Tulsa, 2002, pp. 575-578.
- [9] P.G. Drennan and C.C. McAndrew, “Understanding MOSFET mismatch for analog design,” *IEEE J. Solid-State Circuits*, vol. 38, pp. 450-456, March 2003.
- [10] P. Gray, P. Hurst, S. Lewis, R. Meyer, *Analysis and Design of Analog Integrated Circuits*, John Wiley & Sons, pp. 329.
- [11] B. Abesingha, G. A. Rincón-Mora, and D. Briggs, “Voltage shift in plastic-packaged bandgap references,” *IEEE Trans. Circuits Sys. - II*, vol. 49, pp. 681-685, Oct. 2002.
- [12] V. Ceekala, et. al, “A method for reducing the effects of random mismatch in CMOS bandgap references” in *ISSCC*, vol. 2, pp. 318-319, 2002.
- [13] M. Pertijs, A. Bakker, and J. Huijsing, “A high-accuracy temperature sensor with second-order curvature correction and digital bus interface,” in *ISCAS*, vol. 1, pp. 368-371.